AD-A153 407 LIGHT SCATTERING AND SPECTROSCOPIC STUDIES OF POLYMERIZATION PROCESSES(U) STATE UNIV OF NEW YORK AT STONY BROOK DEPT OF CHEMISTRY B CHU 01 MAR 85 5010D 1/1

UNCLASSIFIED ARO-18675.8-CH DAAG29-82-K-0044 F/G 7/4 NL

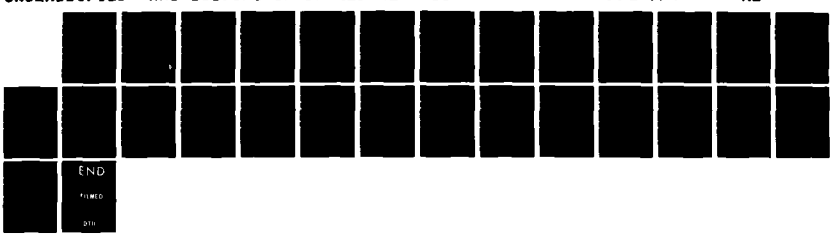

END

FILMED

DTIC

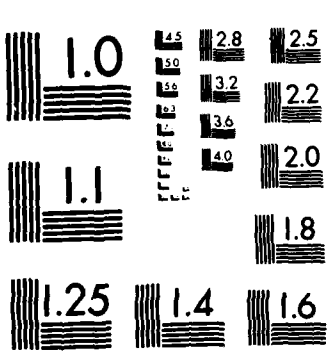

Light Scattering and Spectroscopic Studies of Polymerization Processes

Final Report

Ben Chu

March 1, 1985

U.S. Army Research Office

Contract #DAAG29 82K 0044

Chemistry Department
State University of New York at Stony Brook

REPORT DOCUMENTATION PAGE

READ INSTRUCTIONS BEFORE COMPLETING FORM

1. REPORT NUMBER: ARO 18675.8-CH	2. GOVT ACCESSION NO.: N/A
3. RECIPIENT'S CATALOG NUMBER: N/A	
4. TITLE (and Subtitle): LIGHT SCATTERING AND SPECTROSCOPIC STUDIES OF POLYMERIZATION PROCESSES	5. TYPE OF REPORT & PERIOD COVERED: Final Report 2/1/82 - 1/31/85
	6. PERFORMING ORG. REPORT NUMBER: 5010D
7. AUTHOR(s): Ben Chu	8. CONTRACT OR GRANT NUMBER(s): DAAG29 82K 0044
9. PERFORMING ORGANIZATION NAME AND ADDRESS: Chemistry Department, State University of New York, Stony Brook, New York 11794-3400	10. PROGRAM ELEMENT, PROJECT, TASK AREA & WORK UNIT NUMBERS
11. CONTROLLING OFFICE NAME AND ADDRESS: U. S. Army Research Office, Post Office Box 12211, Research Triangle Park, NC 27709	12. REPORT DATE: March 1, 1985
	13. NUMBER OF PAGES
14. MONITORING AGENCY NAME & ADDRESS (if different from Controlling Office)	15. SECURITY CLASS. (of this report): Unclassified
	15a. DECLASSIFICATION/DOWNGRADING SCHEDULE

16. DISTRIBUTION STATEMENT (of this Report)

Approved for public release; distribution unlimited.

17. DISTRIBUTION STATEMENT (of the abstract entered in Block 20, if different from Report)

NA

18. SUPPLEMENTARY NOTES

The view, opinions, and/or findings contained in this report are those of the author(s) and should not be construed as an official Department of the Army position, policy, or decision, unless so designated by other documentation.

19. KEY WORDS (Continue on reverse side if necessary and identify by block number)

Polymer Characterization, Polymerization Processes, Photon Correlation Spectroscopy and Raman Scattering as macromolecular probes

20. ABSTRACT (Continue on reverse side if necessary and identify by block number)

Raman scattering and laser light scattering have been used to demonstrate the feasibility of spectroscopic techniques to characterize macromolecular properties during polymerization processes in situ. The method could be developed into an on-line probe using fiber optics for monitoring solution and melt polymerization processes in reaction vessels.

DD FORM 1 JAN 73 1473 EDITION OF 1 NOV 65 IS OBSOLETE

A. FOREWARD

I greatly appreciate continued research support by the U.S. Army Research Office since 1963. The long-range views of the program administrators, including their patience and understanding, have contributed substantially toward my success in the laser light scattering field. I am glad to report that new advances in laser light scattering have made the technique an important component in modern polymer materials characterization. In particular, we have extended the application of this technique to investigate polymerization processes at high temperatures, such as the thermal polymerization of hexachlorocyclotriphosphazene, a polymer of interest to AMMRC, Watertown, Mass.

B. List of Publications

During the contract period (2/1/82 - 1/31/85), the following articles were published with total or partial support of DAAG29-82K-0044 administered by the U.S. Army Research Office.

1982. B. Chu and G. Fytas, Light Scattering and Spectroscopic Studies of Polymerization Processes. 2. Thermal Polymerization of Styrene, Macromolecules, 15, 561 (1982).

M.-J. He, K. Kubota, J. Pope and B. Chu, Static and Dynamical Properties of Polystyrene in Carbon Tetrachloride. 3. Effects of Freezing on Solution Properties, Macromolecules, 15, 673 (1982).

1983. K. Kubota and B. Chu, Quasielastic Light Scattering of Poly(hexyl isocyanate) in Hexane, Macromolecules, 16, 105 (1983).

K. M. Abbey, J. Shook and B. Chu, "Correlation Function Profile Analysis in Laser Light Scattering. II. A Hybrid Photon Correlation Spectrometer," in The Application of Laser Light Scattering to the Study of Biological Motion, edited by J. C. Earnshaw and M. W. Steer, Plenum Press, New York (1983) pp. 77-87.

K. Kubota and B. Chu, Laser Light Scattering of PBLG in DMF, Biopolymers, 22, 1461 (1983).

1984. B. Chu and Day-Chyuan Lee, "Characterization of PMMA During the Thermal Polymerization of Methyl Methacrylate," Macromolecules, 17, 926 (1984).

B. Chu, M. Onclin and J. R. Ford, "Laser Light Scattering Characterization of Polyethylene in 1,2,4-Trichlorobenzene, J. Phys. Chem., 88, 6566 (1984).

J. W. Pope and B. Chu, "A Laser Light Scattering Study on Molecular Weight Distribution of Linear Polyethylene," Macromolecules, 17, 2633 (1984).

1985. Benjamin Chu, "Light Scattering Studies of Polymer Solutions and Melts," Polymer Journal, Japan, 17, 225 (1985).

Benjamin Chu, Chi Wu and James R. Ford, "Laser Light Scattering Characterization of Molecular Weight Distribution of Wormlike Chains Poly(1,4-phenylene terephthalamide) in Concentrated Sulfuric Acid," Journal of Colloid and Interface Science, submitted for publication.

Reviews

Publication List (cont'd.)

B. Chu, Correlation Function Profile Analysis in Laser Light Scattering. I. General Review on Methods of Data Analysis, in The Application of Laser Light Scattering to the Study of Biological Motion, edited by J.C. Earnshaw and M.W. Steer, Plenum Press, New York (1983), pp. 53-76.

B. Chu, Light Scattering Studies of Polymer Solution Dynamics, J. Polymer Sci., to be published.

C. Participating Personnel

Post-Doctorates:	James R. Ford
Graduate Students:	Day-Chyuan Lee
	Roger Rodriguez
	Il-Hyun Park
	Renliang Xu
Secretarial:	Jane Wainio

Light Scattering and Spectroscopic Studies of Polymerization Processes

by

Ben Chu
Departments of Chemistry and of Materials Science and Engineering
State University of New York at Stony Brook
Long Island, New York 11794-3400

ABSTRACT

During the thermal polymerization of monomers such as methyl methacrylate (MMA) or styrene, we have been able to investigate both the static and the dynamic properties of the polymer formed, i.e., polymethyl methacrylate (PMMA) or polystyrene, in terms of the molecular weight M_w, the second virial coefficient A_2, the radius of gyration R_g, the translational diffusion coefficient D_T and its corresponding equivalent hydrodynamic radius R_h as well as estimates of the size (or molecular weight) distribution of the polymer in dilute solution; and in terms of the isothermal compressibility $(\partial\pi/\partial C)_{P,T}$, the cooperative diffusion coefficient D_c and a slow characteristic decay time which has sometimes been related to the self-diffusion coefficient D_s in the semidilute solution regime.

By combining a spectroscopic technique, such as Raman scattering, which can determine the polymer concentration non-evasively during the polymerization process, with laser light scattering, we have demonstrated a viable procedure for on-line monitoring of solution polymerization processes permitting us to investigate detailed macromolecular properties in solution polymerization kinetics.

The same approach has been extended to examine the thermal polymerizaion of melt hexachlorocyclotriphosphazine and of hexachlorocyclotriphosphazene in 1,2,4-trichlorobenzene to form poly(dichlorophosphazene).

I. INTRODUCTION

Studies of polymerization processes have been difficult because we lack a convenient probe which we can use on-line to monitor the concentrations of the monomer(s) and of the polymer in a polymerization reaction. Spectroscopic techniques, such as NMR, IR, Raman and fluorescence, and other physical methods, such as density and surface tension, offer reasonable and possible alternatives which permit us to measure the appropriate concentration of species in a chemical reaction. However, in a polymerization process, we really want to know not only the concentrations of the monomer (C_m) and of the polymer (C_p), but also molecular parameters, such as the molecular weight M, of the polymer product during the chemical reaction.

The main aim of this project was directed at an important need in chemical reactor engineering, i.e., we tried to link together an application of several established results in Raman scattering and laser light scattering and hopefully to demonstrate that development of an on-line technique for characterizing the polymer product during the course of the polymerization reaction was a worthwhile undertaking.

It should be recognized that our measurement scheme is limited mainly to solution and bulk polymerization processes and that we have neglected convective motions which often exist in a chemical reactor. Such convective motions which could be produced by flow of reactant(s) and product(s) and/or by thermal gradients would invariably affect the light scattering spectrum and the translational diffusive motions of the polymer product(s). However, these problems may be resolved by varying experimental conditions or they can be investigated for specific systems. For example, flow can be measured using laser Doppler velocimetry[1] and thermal gradients can be alleviated by changing the chemical reaction vessel design.

In the final report, we summarize the results of our studies on the thermal polymerization of a monomer, e.g. methyl methacrylate (MMA) using a combination of Raman scattering and laser light scattering[1] whereby we have been able to measure many of the main variables of interest in terms of known molecular parameters, namely, the rate of conversion, the weight average molecular weight M_w of the polymer product, polymethyl methacrylate (PMMA), and estimates of the polymer polydispersity. Furthermore, due to the specific nature of the polymerization process, i.e., for free radical polymerization, we know the molecular weight of the polymer formed to remain relatively constant, we have been able to establish Zimm plots in dilute solutions and to determine both the second virial coefficient A_2 and the radius of gyration R_g in addition to the weight average molecular weight. In the same dilute solutions, precise measurements of the time correlation function permit us to determine the z-average translational diffusion coefficient D_T, its corresponding equivalent hydrodynamic radius R_h, and the polydispersity index $(\mu_2/\bar{\Gamma}^2)$ as well as to estimate the linewidth distribution function $G(\Gamma)$ which is related to the hydrodynamic size (or the molecular weight) distribution. At higher solution concentrations in the semi-dilute regime, we have succeeded in determining the osmotic compressibility $(\partial\pi/\partial C)_{P,T}$ and the cooperative diffusion coefficient D_c and in confirming the existence of a very slow characteristic decay time which has been related to the self-diffusion coefficient D_s as a function of concentration (time). As the very slow characteristic decay time has a molecular weight dependence, more careful time correlation function profile analysis also suggests a scheme whereby we can estimate molecular (or clustering) polydispersity from a correlation function profile analysis of the slow mode in semidilute solutions. It should be emphasized that our development of a practical concentration and molecular parameter probe for polymerization process control is still in progress. The present report is concerned mainly with the potential of such a scheme.

II. THEORETICAL RATIONALE

Light scattering and Raman spectroscopic techniques have been used to study the thermal polymerization of styrene[2,3] and of MMA.[4] The techniques are non-invasive and can share the same light source and detection electronics.

II.1. Raman Spectroscopy

Raman spectroscopy has been a useful tool to elucidate the structure of polymers. In a chemical reaction, some bonds are broken and others are being formed while most remain relatively unchanged. Therefore, Raman peaks which are characteristic of the respective chemicals of interest can be used to

monitor the concentrations of those chemicals, while the peaks which show no change during the polymerization process can be used to monitor the laser incident intensity and act as some form of an internal built-in reference standard useful for normalization purposes. On closer examination, Raman polymer peaks may depend on other factors in addition to polymer concentration and the location and shape of Raman peaks may change slightly due to structural variations during the polymerization process. Therefore, in using the Raman spectroscopic technique as a probe to monitor concentration of chemical species, we should also use other analytical analysis to confirm the scheme.

II.2. Intensity of Scattered Light[5]

The Rayleigh ratio (R_{vu}) for vertically polarized incident and unpolarized scattered light at finite concentrations in dilute solution has the approximation form:

$$\frac{HC}{R_{vu}} = (M_w^{-1} + 2A_2C)\left(1 + \frac{16\pi^2 n^2}{3\lambda_o^2} R_g^2 \sin^2\left(\frac{\theta}{2}\right)\right) \qquad (1)$$

where H, in units of mole $cm^2 g^{-2}$, is equal to $4\pi^2 n^2 (\partial n/\partial C)^2/(N_A \lambda_o^4)$ with n, $C(g/cm^3)$, N_A, λ_o, $\partial n/\partial C$ being the respective refractive index, concentration, Avogadro's number, wavelength in vacuo, and refractive index increment; R_{vu} (cm^{-1}) is the excess Rayleigh ratio due to concentration fluctuations of the polymer solution using vertically polarized incident and unpolarized scattered light; M_w (g $mole^{-1}$) is the weight-average molecular weight, A_2 (moles cm^3 g^{-2}) is the second virial coefficient and R_g (cm) is the root mean square radius of gyration.

According to eq. (1), the second virial coefficient A_2, the weight-average molecular weight M_w and the radius of gyration R_g can be determined using a Zimm plot whereby

$$\lim_{C\to 0} \frac{HC}{R_{vu}} = \frac{1}{M_w}\left(1 + \frac{K^2 R_g^2}{3}\right), \qquad (2)$$

$$\lim_{\theta\to 0} \frac{HC}{R_{vu}} = \frac{1}{M_w} + 2A_2C, \qquad (3)$$

and

$$\lim_{\substack{C\to 0 \\ \theta\to 0}} \frac{HC}{R_{vu}} = \frac{1}{M_w}. \qquad (4)$$

where $K[=(4\pi/\lambda)\sin(\theta/2)$ with $\lambda = \lambda_o/n]$ is the magnitude of the momentum transfer vector. Eq. (1) is no longer valid at higher concentrations. However, we can write

$$\lim_{K\to 0} \frac{HC}{R_{vu}} = \frac{1}{RT}\left(\frac{\partial \pi}{\partial C}\right)_{T,P} \qquad (5)$$

where the concentration dependent osmotic compressibility term, $(\partial\pi/\partial C)_{T,P}$, is independent of the polymer molecular weight, at least for specific polymer solutions in a good solvent.

II.3. Spectrum of Scattered Light[5,6]

The measured single-clipped photoelectron count autocorrelation function for a detector of finite effective photocathode has the form:

$$G_k^{(2)}(\tau) = N_s\langle n_k\rangle\langle n\rangle(1 + b|g^{(1)}(\tau)|^2) \qquad (6)$$

where $g^{(1)}(\tau)$ is the first-order normalized time correlation function of the scattered electric field, k is the clipping level, τ is the delay time, $\langle n_k\rangle$ and $\langle n\rangle$ are mean clipped and unclipped counts per sample time, and $\langle N_s\rangle$ is the total number of sample with the baseline $A = N_s\langle n_k\rangle\langle n\rangle$. $N_s\langle n_k\rangle$ and $N_s\langle n\rangle$ are the total clipped counts and total unclipped counts, respectively. b is a spatial coherence factor depending upon various experimental conditions, such as coherence and receiver areas and is usually taken as an unknown parameter in the data fitting procedure. Eq. (6) is valid for an extensive class of signals having Gaussian field probability distribution.[6]

For a monodisperse sample of non-interacting macromolecules in solution (or colloidal particles in suspension):

$$\sqrt{Ab}\, g^{(1)}(K,\tau) \propto I(K)\exp(-\Gamma(K)\tau) \qquad (7)$$

where the scattered intensity $I(K) = Ni(K)$, with N and i being the number of macromolecules in the scattering volume V and the scattered intensity from each macromolecule, respectively. Γ ($= D_T K^2$ when $KR_g << 1$) is the characteristic linewidth with $D_T(cm^2sec^{-1})$ being the translational diffusion coefficient. At finite but dilute concentrations and in the presence of interactions

$$D = D_o(1+k_dC) \qquad (8)$$

where D_o is the diffusion coefficient at infinite dilution. The hydrodynamic and thermodynamic factors are combined in the second virial coefficient for diffusion k_d which is system specific.

In semidilute solution and in the small KR_g range which avoids the complication of internal polymer motions, the time correlation function measures the cooperative diffusion coefficient D_c and another much slower relaxation time which has been related to the self-diffusion coefficient D_s.[7-9] Identity of this slow relaxation time to D_s has been open for discussion. It is suffice to say that the measured slow relaxation time can be utilized to characterize molecular (or clustering) properties of the

polymer product formed in semidilute solutions regardless of the source of discrepancy. Generally we can express D_c and D_s to be in their respective pseudogel ($K\xi_c << 1$) and reptation ($KR_g << 1$) regimes with ξ_c being the screening length of concentration blobs. The cooperative diffusion coefficient is independent of molecular weight and is proportional to $C^{3/4}$ and C^1 in semidilute-good and semidilute-theta solvents, respectively. On the other hand, the slow mode which mimics the self-diffusion coefficient depends on the molecular weight and we have, according to the scaling concept:

$$\begin{aligned} D_s &= k_s M^{-2}C^{-7/4} \quad \text{semidilute-good region, and} \\ D_s &= k_s^* M^{-2}C^{-3} \quad \text{semidilute-theta region} \end{aligned} \tag{9}$$

with k_s and k_s^* being proportionality constants. Therefore, under appropriate conditions, perhaps eq. (9) can suggest a scheme to calibrate the molecular weight and its polydispersity of the polymer product at semidilute concentrations. The suggestion, however, has not been explored experimentally.

II.4. Correlation Function Profile Analysis[10-12]

For a polydisperse sample,

$$|g^{(1)}(\tau)| = \int_0^\infty G(\Gamma)\exp(-\Gamma\tau)d\Gamma \tag{10}$$

where $G(\Gamma)$ is the normalized distribution of decay rates. In practice, eq. (10) uses a measured $|g^{(1)}(\tau)|$ which has noise and is bandwidth limited. Furthermore, the limits of integration have both upper and lower bounds yielding

$$|g^{(1)}(\tau)| = \int_a^b G(\Gamma)\exp(-\Gamma\tau)d\Gamma \tag{10'}$$

As the Laplace transform of eq. (10') is ill-conditioned, we can only approximate $G(\Gamma)$ using methods which can put further constraints to the problem. We have considered the multiexponential approach with solutions to be evaluated by the singular-value decomposition method.[11] We approximate $G(\Gamma)$ as a sum of equally spaced single exponentials

$$G(\Gamma) \propto \sum_{j=1}^{m} I_j \delta(\Gamma - \Gamma_j) \tag{11}$$

or as a sum of logarithmically spaced single exponentials

$$G(\Gamma) \propto \sum_{j=1}^{m} I_j^* \delta(\ell n\Gamma - \ell n\Gamma_j) \tag{12}$$

where m is a small number, usually 3 or 4, depending upon the signal-to-noise ratio of $g^{(1)}(\tau)$ and the b/a ratio. The superscript * signifies a change of variable from Γ to ℓn. According to eq. (4) and $I(K) = Ni(K)$, we have

$$N_j(M_j) \propto I_j(M_j)/M_j^2 \tag{13}$$

where $_j(M_j)$ is the number of <u>representative</u> (discrete) polymer molecules with

molecular weight M_j and $I_j(M_j)$ is the corresponding scattered intensity from N_j polymer molecules. In eq. (13), we have taken the limit of $K \to 0$ and $C \to 0$. In dilute solution, first order correction due to the contributions from $P(KR_g)$ and A_2 can be introduced. Then, we have

$$N_j(M_j) \propto \frac{I_j(M_j)[1+K^2 R_{g,j}{}^2(M_j)/3 + 2\bar{A}_2 C M_j]}{M_j^2} \tag{14}$$

where we have taken $P^{-1} \approx 1 + K^2 R_g{}^2/3$ and $\bar{A}_2$ to be the measured second virial coefficient over the concentration range of eq. (1).

Having obtained an estimate of the normalized distribution of translational diffusion coefficient G(D), we define the number molecular weight distribution:

$$F_n(M_j) = \sum_{j=1}^{m} N_j \, \delta(M-M_j) \tag{15}$$

and relate each representative translational diffusion coefficient, D_j, with a molecular weight, M_j, and a characteristic molecular parameter, $X_j(\equiv KR_{g,j})$, by use of the following molecular weight scaling laws[13] for D and R_g

$$D = k_D M^{-\alpha_D} \tag{16}$$

$$R_g = k_R M^{\alpha_R} \tag{17}$$

The two scaling laws are also closely tied to the intrinsic viscosity scaling law exponent such that if $[\eta] = k_\eta M^{\alpha_\eta}, \alpha_D = (1+\alpha_\eta)/3$. We can evaluate the pre-exponential factors k_D and k_R by using the measured values of M_w and R_g from static light scattering studies provided that α_D and α_R are known. In the iterative procedure, we first estimated k_D by assuming that $P(X) = 1$ and then adjusted k_R by comparing the measured and computed R_g values using the first approximate $F_n(M_j)$. We then vary k_D by comparing the measured and computed values of M_w. The iterative procedure was terminated when a k_D value could yield an $M_{w,calc}$ which was in agreement with the measured M_w from our static light scattering measurements. For completeness we note that

$$M_{w,\,calc} = \Sigma N_j M_j{}^2 / \Sigma N_j M_j \tag{18}$$

$$R_{g,calc} = k_R \, \Sigma N_j M_j{}^{(2+\alpha_R)} / \Sigma N_j M_j{}^2 \tag{19}$$

and

$$F_{w,cum} = \int_M^\infty F_n(M) M \, dM / \int_M^\infty F_n(M) M \, dM \tag{20}$$

where $F_{w,cum}(M)$ is the normalized cumulative weight-average molecular

weight distribution.

III. EXPERIMENTAL METHODS

Raman spectra were obtained using a Spex 1302 double monochrometer (0.5 meter, 1200 grooves/mm). The Raman spectrometer was modified to accept a high temperature cell for the thermal polymerization of MMA and to measure the absolute light scattering intensity and spectrum at four different scattering angles. Both Raman scattering and light scattering intensity measurements were recorded and controlled by a HP 9830 calculator. We used an argon ion laser operating at 488.0 nm as the incident light source for both Raman and light scattering measurements. Integrated scattered intensities were measured by a standard photon-counting detection system while the single-clipped photoelectron count autocorrelation function was measured with a Malvern K7023 correlator. Temperatures were controlled to $\pm 0.01^{\circ}C$ near room temperature and to $\pm 0.05^{\circ}C$ at high temperatures.

Among the three samples we used as illustrations, #2 was degassed by several freeze-pump cycles with the inhibitor (hydroquinone monomethyl ether) being left undisturbed. Both #1 and #3 were first distilled, adding one drop of mother undistilled MMA in order to introduce a trace amount of the inhibitor, and then degassed. The trace amount of inhibitor provided time for us to manipulate the MMA before polymerization reaction could start. All solutions were filtered through a Millipore filter of nominal 0.22 μm pore diameter before measurements.

We used benzene as a reference for computing the Rayleigh ratio R_{vu} and took $R_{vu} = R_{vv} + R_{vh} = 3.86 \times 10^{-5}$ cm^{-1}[14] for benzene at $\theta = 90^{\circ}$, $\lambda_o = 488$ nm and $23^{\circ}C$.

The refractive index of MMA at $\lambda_o = 488$ nm was estimated to be 1.3731 and 1.3999 at 90° and $50^{\circ}C$, respectively. The refractive index increment was determined using a Brice Phoenix differential refractometer. By extrapolation, we estimated $\partial n/\partial C = 0.100$ at $90^{\circ}C$ and $\partial n/\partial C = 0.0838$ at $50^{\circ}C$ for $\lambda_o = 488.0$ nm. The density of MMA and of PMMA were adapted from the Polymer Handbook which showed values of 0.880 and 0.918 g/cm^3 for MMA and values of 1.171 and 1.182 g/cm^3 for PMMA at 90° and $50^{\circ}C$, respectively. The viscosities of MMA have values of 0.26 and 0.42 cP at 90° and $50^{\circ}C$, respectively.

IV. RESULTS AND DISCUSSION

Raman spectra were used to determine the concentration of the reactant (monomer) and of the product (polymer). From the product formed as a function of time, we can study the kinetics of polymerization processes in terms of conversion and the Trommsdorf effect. In dilute solutions, we can make full use of light scattering intensity and linewidth data to obtain many of the pertinent molecular parameters of the polymer formed during the polymerization process.

IV.1. Raman Spectra

We first measured the Raman spectra of the monomer MMA and of the polymer PMMA. We then selected the 1732 cm^{-1} peak due to the carbon-oxygen double bond (C=O) stretching as our internal standard and the aliphatic carbon-carbon double bond (C=C) at 1639 cm^{-1} as a probe for the monomer concentration. Figure 1 shows several Raman spectra obtained during the thermal

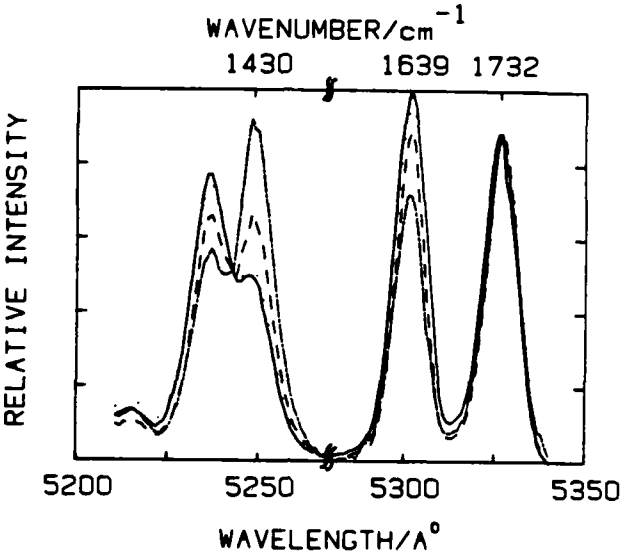

Fig. 1. Several Raman spectra obtained during the course of thermal polymerization of MMA at 50°C showing the decrease in C=C peak at 1639 cm^{-1} and the constant intensity in the C=O peak at 1732 cm^{-1} for sample #3 at 13 hr. (solid spectrum) 54.5 hr. (dotted spectrum) 266 hr. (dashed spectrum) and 351 hr. (dash-dot line). A more complex polymer peak at 1430 cm^{-1} is not being evaluated in this study partly because the polymer peak may depend on macromolecular properties, partly because we have been interested in conversion studies up to <50% completion before the laser incident intensity damages the polymer glass being formed, and partly because of its overlap with another monomer peak.

polymerization of MMA at 50°C. The decrease in the C=C peak at 1639 cm^{-1} with increasing time shows that the monomers are being used up during the polymerization process while the relatively constant peak of the C=O bond at 1732 cm^{-1} confirms that our entire light scattering system has remained stable over extended periods of time, i.e., over a period of 15 days. Laser intensity stability is not an important issue here because we can always use the internal reference, C=O peak, to normalize the intensities of other peaks of interest. It was not necessary to have the laser on during the entire course of the experiment. The polymer peak at 1430 cm^{-1} reveals the formation of PMMA. However, in the initial stages, the appearance of a polymer peak has relatively low signal-to-noise advantages. So, a direct determination of the polymer concentration is more difficult to detect from the appearance of a Raman peak when the polymer concentration is low. Furthermore, it is not

certain whether this polymer peak is independent of its molecular properties and depends only upon the polymer concentration. The overlapping neighboring monomer peak may also affect our evaluation of the polymer peak. It should be recognized that the polymer peak could yield useful information as the polymerization process progresses towards its complete conversion. However, we have not used the polymer peak in our present study.

In the Raman spectra, we have observed that the shape of the Raman peaks and the half-width of the monomer characteristic peak at 1639 cm^{-1} as well as that of the C=O bond stretching at 1732 cm^{-1} remains relatively unchanged. Although the fractional conversion of the monomer can best be determined using the ratio of the integrated peak area of the C=C stretching intensity at 1639 cm^{-1} to that of the C=O reference peak at 1732 cm^{-1}, we have used the C=C peak height h_m and normalized it by the C=O peak height h_r in order to obtain the fractional conversion of the monomer f_m and the fractional conversion of the polymer f_p (= $1-f_m$) with

$$f_m(t) = \frac{h_m(t)}{h_r(t)} \cdot \frac{h_r^o}{h_m^o} \tag{21}$$

where the superscript zero represents the peak height values at t=0. The concentration of polymer formed, $C_p(g/cm^3)$, has the form:

$$C_p = \frac{f_p d_m d_p}{f_p d_m + f_m d_p} \tag{22}$$

where d_p and d_m are densities of PMMA and of MMA, in g/cm^3, respectively. In eq. (22), we have assumed no interaction between PMMA and MMA, i.e., volume of mixing is zero. A typical plot of initial fractional conversion of monomer as a function of time can be represented by

$$f_p = 1 - \exp(-a_1 t) \tag{23}$$

with the numerical values for a_1 listed in Table 1. Samples #2 and #3 were reacted at 50°C mainly for our own convenience because the lower reaction temperature permits us to have ample time to carry out our light scattering linewidth measurements and to check for reproducibility. Figure 2 shows plots of fractional conversion of monomer versus time for samples #2 (with a large amount of inhibitor) and #3 (with only a trace amount of the inhibitor from one drop of undistilled MMA) at 50°C. The induction period (much longer for sample #2) has been omitted in the plots. It should be noted that the reaction rate is affected by the amount of inhibitor in MMA. This is one of the reasons why the proposed scheme will be useful for monitoring polymerization processes.

We have arbitrarily separated the polymerization process into two parts. The linear behavior with a constant reaction rate is represented by eq. (23). A rapid increase occurs at about 5% of f_p for the thermal polymerization of MMA at 50°C. The acceleration due to the "gel effect" has often been referred

to as the Trommsdorf effect which is accompanied by high viscosities. The relationship between the onset of the autoacceleration rate and solution properties of the monomer-polymer system has been discussed by many authors[15-18] We shall use only a simple kinetic scheme[19] to represent the polymerization of MMA as shown in Fig. 2:

$$\ell n[(f_p-a_2)/(a_3-f_p)] = a_4 + a_5 t \qquad (24)$$

where a_i's are the appropriate constants. The results are summarized in Table 1.

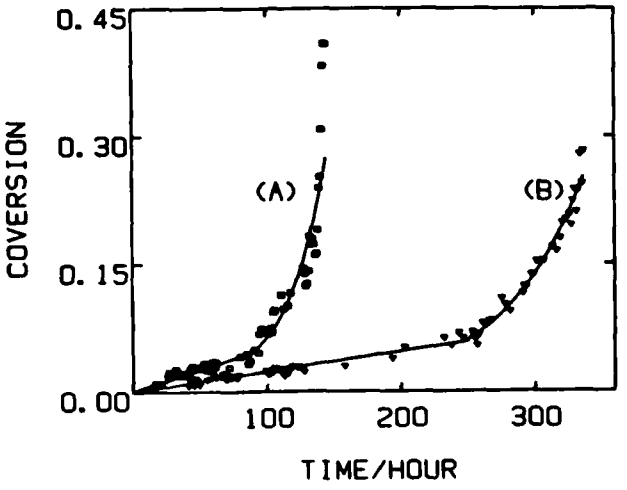

Fig. 2. Fractional conversion of monomer versus time obtained from the height change of C=C peak for sample #2 (□, experimental data; solid line A, fitted curve) and sample #3 (▽, experimental data; solid line B, fitted curve) at 50°C). The solid lines A and B for samples #2 and #3 were fitted according to eqs. (23) and (24) with numerical values listed in Table 1. We have arbitrarily separated the results into two parts: one before gel effect (eq. (23)) and the other in in the presence of gel effect. The longer induction period for sample #2 due to the presence of a much larger amount of the inhibitor is not shown.

IV.2. Intensity of Scattered Light

By means of eqs. (22)-(24), we can determine the polymer concentration Cp at any time during the polymerization process. We shall now combine this information with light scattering (intensity) measurements to examine the molecular properties of the polymer product(s) formed. The intensity of scattered light at four different scattering angles (35, 60, 90 and 135°) were measured. By extrapolation to zero scattering angle and subtracting the scattered intensity of MMA, we have determined $R_{vu}(\theta=0)$ as a function of

concentration. Sample #1 (90°C) exhibits intensity behaviors slightly different than those of samples #2 and #3 (both at 50°C). For example, the maximum for sample #1 occurs at a slightly higher concentration than those of samples #2 and #3. We shall return to this data set after we have made an analysis first in dilute solutions.

Table 1
Conditions and fitting parameters in evaluating the time dependence of fractional conversion of monomer during the thermal polymerization of MMA

Sample #	1	2	3
Conditions (all samples were degassed)	distilled + one drop of undistilled MMA	undistilled MMA (with inhibitor)	distilled + one drop of undistilled MMA
Temperatures (°C)	90	50	50
a_1 (hr^{-1})	1.72×10^{-3}	4.85×10^{-4}	2.43×10^{-4}
a_2 (g/cm^3)		1.44×10^{-2}	6.25×10^{-3}
a_3 (g/cm^3)		6.89	2.67
a_4		-9.04	-8.45
a_5 (hr^{-1})		4.01×10^{-2}	1.83×10^{-2}

Note: $f_p = 1 - \exp(-a_1 t)$ (23)

$$\ell n \frac{(f_p - a_2)}{(a_3 - f_p)} = a_4 + a_5 t \qquad (24)$$

In a free radical polymerization process we know that the polymer molecular weight remains relatively constant during the initial polymerization process. So in a Zimm plot as illustrated typically in Fig. 3 for sample #1, we can determine the molecular weight, M_w, the second virial coefficient A_2, and the radius of gyration R_g, of the polymer product(s) formed according to eqs. (1)-(4). The polymer concentration C_p was determined by means of eqs. (22)-(24) using conversion data of Fig. 2 from Raman scattering. The results are summarized in Table 2. The linear behavior in the Zimm plots strongly suggests our supposition that the molecular weight of the polymer indeed remains constant. In semidilute solutions, we may want to examine the static property of the polymer solution in terms of $M(\partial\pi/\partial C)/RT$ as a function of reduced concentration C/C^* where C^* ($\equiv M/N_A R_g^3$) is the overlap concentration as shown in Fig. 4 and Table 2. The universal curve in the molecular weight range which we have illustrated can be represented by straight lines over limited ranges in the semidilute solution regime, as shown in Fig. 4.

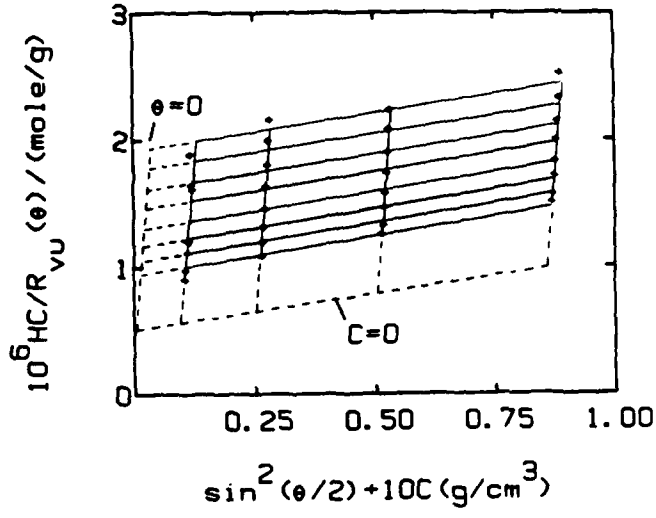

Fig. 3. Zimm plot for sample #1. Distilled MMA + one drop of undistilled MMA (representing introduction of a trace amount of inhibitor) thermal polymerized at 90°C.

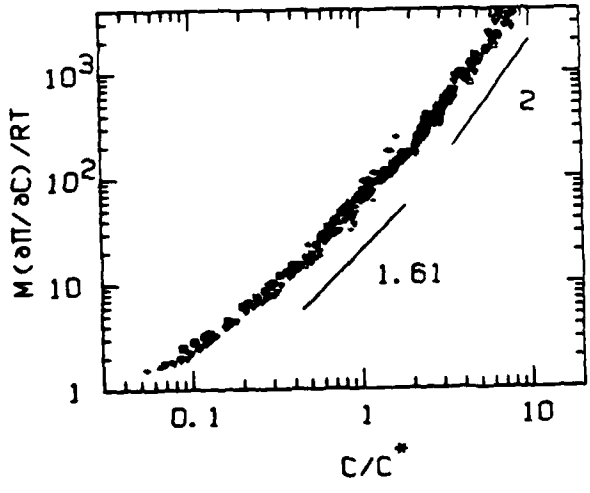

Fig. 4. Log-log plot of $M(\partial\pi/\partial C)/RT$ versus C/C^* for sample #1 (plus signs), sample #2 (hollow squares) and sample #3 (inverted hollow triangles).

Measurements of the osmotic compressibility in semidilute solutions permit us to determine the polymer concentration independent of the polymer molecular weight. The solid straight line in Fig. 4 can be represented by $M(\partial\pi/\partial C)/RT = k_M(C/C^*)^m$ where m varies from an initial slope of 1.5 at low ranges of C/C^* (<1) to ~2 for $C/C^* > 2$. According to the scaling law, $m = 1/(3\alpha_R - 1) = 1.5$ and 2 for $\alpha_R = 0.56$ and 0.50, respectively. The cross-over region is very broad from dilute to semidilute concentrations. We note that in the limit of zero concentration, eqs. (4) and (5) combine to yield $\lim_{C\to 0}(\partial\pi/\partial C)/RT = 1/M_w$.

Table 2
Moleular parameters in dilute solution

Sample	M_w(g/mole)x10^{-6}	A_2(mole cm^3g^{-2})	R_g(nm)	C^*(g/cm^3)
#1	2.00	$2.0x10^{-4}$	52.2	$2.33x10^{-2}$
#2	3.70	$1.8x10^{-4}$	74.5	$1.49x10^{-2}$
#3	4.54	$1.5x10^{-4}$	84.5	$1.24x10^{-3}$

Therefore, the universal curve in Fig. 4 starts at values very slightly higher than 1 in dilute concentrations and it increases with increasing concentration because of a positive A_2 in good solvent, such as our system of PMMA in MMA. However, A_2 is related to M and C^*. So, the universal curve is valid over the entire concentration range from dilute to semidilute solutions including the cross-over region. More quantitative behavior using renormalization group techniques have been reported.[20] In fairly good solvents, Fig. 4 can be used to extract the polymer concentration from measurements of absolute scattered intensity at zero scattering angle ($R_{vu}(\theta\to0)$) provided that the refractive index increment of the polymer/solvent system is known. While theory deals mainly with monodisperse polymers, an experiment on the thermal polymerization of MMA yields PMMA with a fairly polydisperse distribution, i.e., $M_w/M_n \sim 2$. In constructing this particular universal curve we have implicitly assumed that the polydispersity effect is negligible since π is independent of molecular weight in semidilute solutions. The fact that the data points do overlap suggest that it is valid for us to make such approximations. Furthermore, the agreement between the theoretical and the experimental value for m at $C/C^* \sim 1$ strengthens our suppositions which will again be verified by our light-scattering linewidth measurements. It should be noted that once we have demonstrated such a universal curve from experiments, its utility is not restricted to PMMA in MMA. Changes of polydispersity will invariably affect the cross-over region in the universal curve; but the application can certainly be expanded to polymer products with fairly constant broad molecular weight distributions.[20] In Fig. 4, the universal curve is likely to break down if we try to approach the theta condition or to go below the theta temperature for high molecular weight polymers where we may encounter critical effects in the cross-over region,[21] because in this simple scaling plot we have not fully taken into account all of the effects due to solvent quality. We may also construct a log-log plot of $(\partial\pi/\partial C)/RT$ vs C as a function of M as shown in Fig. 5 where we have demonstrated how M can be determined from such a surface in dilute solutions if $(\partial\pi/\partial C)/RT$ and C are known.[3] At constant temperature, Fig. 5 can be collapsed to one universal curve as shown in Fig. 4 over the entire concentration range from dilute to semidilute solutions. The experimental surface as shown in Fig. 5 becomes parallel to the molecular weight axis in semidilute solutions indicating $(\partial\pi/\partial C)_{P,T}$ to be essentially independent of molecular weight.

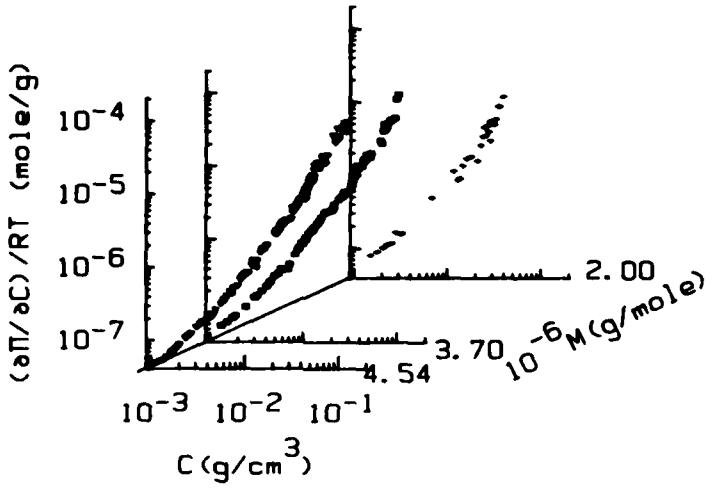

Fig. 5. A three dimensional plot of osmotic compressibility $(\partial\pi/\partial C)_{P,T}$ as a function of concentration and molecular weight for PMMA in MMA, see also Fig. 1 of reference 3 for polystyrene in transdecalin at 45°C. It should be recognized that the osmotic compressibility becomes independent of polymer molecular weight in semidilute solutions. Therefore, the log $(\partial\pi/\partial C)_{P,T}$ versus log C versus M surface is parallel to M in semidilute solutions.

IV.3. Spectrum of Scattered Light

In the initial analysis, we used the second-order cumulants method[22] with

$$Ab|g^{(1)}(\tau)|^2 \cong Ab\ \exp\{2[-\bar{\Gamma}\tau + (1/2)(\mu_2/\bar{\Gamma}^2)(\bar{\Gamma}\tau)^2]\} \qquad (25)$$

where $\mu_2 = \int G(\Gamma)(\Gamma-\bar{\Gamma})^2\, d\Gamma$ and $\bar{\Gamma} = \int G(\Gamma)\Gamma d\Gamma$. In dilute solutions, we have made single exponential, cumulants and multiexponential analysis. The D_T and $\mu_2/\bar{\Gamma}^2$ values are and should be in reasonable agreement using the method of cumulants and the multiexponential model because both approaches try to take into account the polydispersity effect. However, in view of the broader size distributions, there are more uncertainties associated with the second-order cumulants method because we cannot use only the $\bar{\Gamma}$ and μ_2 terms to force fit the time correlation function $|g^{(1)}(\tau)|$ of a fairly polydisperse polymer solution. For polydisperse polymer solutions the single exponential model does not represent the measured time correlation function and it can only be used as an estimate to other more complex models.

In semidilute solutions, the faster cooperative diffusion coefficient D_c is independent of molecular weight and can be fitted using a single exponential function while D_s depends upon molecular weight as shown by eq. (9). Furthermore, as R_g = 84.5 nm, KR_g = 2.15 at $\theta = 90^\circ$ for sample #3,

we assumed that the structure factor correction[23] for internal motions of polymer coils in dilute solution is applicable to $\bar{D}_s$ in semidilute solutions and write

$$\bar{\Gamma}_s = K^2\bar{D}_s(1 + fR_g^2K^2 + \ldots) \qquad (26)$$

where f = 1/5 and 1/6 without and with preaveraging of the hydrodynamic interactions for linear polydisperse polymer coils with a Flory "most probable" distribution. From eq. (26), we get $\bar{D}_s = 2.22\times10^{-9}$ and 2.23×10^{-9} cm^2/sec at $\theta = 35^\circ$ and 90° respectively, and $C = 6.72\times10^{-3}$ g/cm^3 using f = 1/6 and R_g = 84.5 nm at both scattering angles. For sample #3, $C^* = 1.25\times10^{-2}$ g/cm^3 which is greater than $C = 6.72\times10^{-3}$ g/cm^3. However, for polymer viscoelastic fluids, we have the cross-over concentration C_e, representing the onset of entanglement behavior. In theta solutions, $C_e < C^*$.

In computing D_s from correlation function measurements obtained at $\theta = 90^\circ$, we have found $f \approx 1/6$ to be a reasonable correction factor for eq. (26). The second-order cumulants method is approximately valid in the evaluation of $\bar{D}_s$ because we have observed a fairly large variance for D_s. We may conclude from our analysis that the entanglement concentration in shear viscosity, C_e, describes a better dynamical cross over regime from Rouse-like motions to reptation because $\bar{D}_s$ and $\bar{D}_c$ can be measured below C^*, that the power law is valid only over a very limited concentration range in semidilute solutions, because the curves are not really straight lines, and that according to Fig. 4, a log-log plot of $M(\partial\pi/\partial C)/RT$ versus C/C^* exhibits universal behavior over the entire concentration range including cross-over regions from dilute to semiconcentrated solutions.

IV.4. Molecular Weight Distribution Analysis

In dilute solution, we can relate the linewidth distribution function to the molecular weight distribution function.[12,24] So, it is worthwhile to make an approximate Laplace transform of $g^{(1)}(\tau)$ using the multiexponential model. By means of the singular value decomposition technique, we can obtain an approximate $G(\Gamma)$. By taking into account intraparticle interference and concentration effects, we get a plot of $G(D_o)$ versus D_o which can be transformed into a plot of $F_{w,dif}$ versus M where $F_{w,dif}$ is the polymer differential molecular weight function with an "assumed" $\alpha_D = 0.56$ as has been justified indirectly in Table 3. Fig. 6 shows the molecular weight distributions of PMMA obtained by thermal polymerization of MMA with different amounts of inhibitors (samples #2 (dash-double dot curve) and #3 (solid curve) with $\alpha_D = 0.56$). The consistency of our results can best be expressed in Table 4 which shows effects of α_D values on the polydispersity index M_w/M_n. For $\alpha_D \sim 0.55$, $M_w/M_n \sim 2$ for samples #2 and #3, in good agreement with the theoretical prediction of 2 for the thermal polymerization of MMA in the dilute solution region. Figure 7 shows cumulative molecular weight distribution $F_{w,cum}$ based on the results of Fig. 6. The molecular weight of PMMA varies over a range of about 30. It should be recognized that the value of M_w/M_n increases with decreasing α_D values as listed in Table 4. With small variations in α_D, such as 0.54 ~ 0.56, the results of our studies remain unchanged.

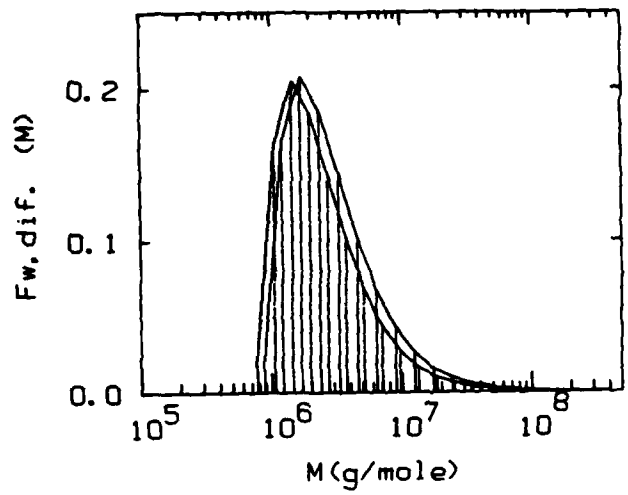

Fig. 6. Molecular weight distributions for samples #2 (dash-double dot curve) and #3 (solid curve) with α_D = 0.56.

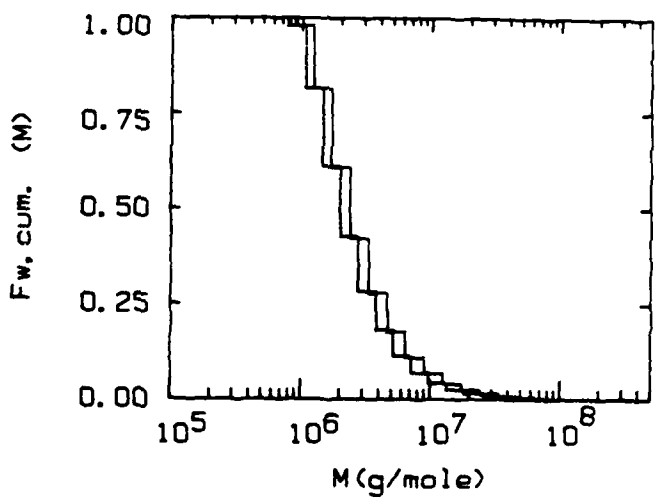

Fig. 7. Cumulative molecular weight distributions for samples #2 (dash-double dot histogram) and #3 (solid histogram) based on the analysis of Fig. 6.

Table 3

Numerical values of limiting slopes according to scaling laws for osmotic compressibility, cooperative diffusion coefficient and self-diffusion coefficient

$M(\partial\pi/\partial C)/RT = k_M(C/C^*)^m$ with $m = 1/3\alpha_R - 1)$

$\overline{D}_s = k_s M^{-2} C^{(\alpha D-2)/(3\alpha-1)}$ (9)

$D_c = k_c C^{\alpha_D/(3\alpha D-1)}$

α_R	m	Observed slope in Fig. 7 for $C/C^* < 1$.
0.5	2	
0.54	1.61	1.61
0.6	1.25	

α_D	$(\alpha_D-2)/(3\alpha_D-1)$	Observed slopes in Fig. 10
0.5	-3	
0.54	-2.36	-2.36
0.6	-1.75	

α_D	$\alpha_D/(3\alpha_D-1)$	
-0.5	1	
-0.54	0.87	0.87
-0.6	0.75	

Table 4

Effects of $_D$ on the polydispersity index M_w/M_n

α_D	M_w/M_n	
	Sample #2	Sample #3
0.50	2.08	2.19
0.52	2.01	2.14
0.54	1.97	2.07
0.56	1.91	2.01
0.58	1.87	1.96
0.60	1.82	1.91

V. Conclusions

We have investigated many of the macromolecular parameters of PMMA in MMA during the thermal polymerization of MMA using a combination of Raman spectroscopy and laser light scattering. In the process, we have made use of the scaling concept to interpret the experimental data as well as the experimental data to support some aspects of the scaling theory. Our results are internally consistent in terms of the concentration behavior of osmotic compressibility, cooperative diffusion coefficient and the very slow characteristic relaxation time (which mimics D_s). In dilute solutions, we have been able to determine the molecular weight distributions of PMMA as well as M_w, A_2, R_g and k_D, provided that the PMMA molecular weight has remained relatively constant during the polymerization process. The linear concentration dependence in osmotic compressibility $(\partial\pi/\partial C)_{T,P}$ and the translational diffusion coefficient D_T seems to strengthen this supposition. Thus, we have demonstrated a scheme whereby we can indeed investigate pertinent macromolecular parameters during solution polymerization kinetics.

In semidilute solutions, we have experimentally observed the slow mode at concentrations below $M_w/(N_A R_g^3)$ suggesting that the overlap concentration C_e is the more appropriate parameter. As the osmotic pressure becomes independent of molecular weight in semidilute solutions, we cannot use the osmotic compressibility to determine the polymer molecular weight. On the other hand, the universal curve in a plot of $(\partial\pi/\partial C)_{P,T}$ versus C in semidilute solutions suggests that we can determine the polymer concentration in semidilute solutions by measuring only the osmotic compressibility. The universal curve in a plot of $M(\partial\pi/\partial C)_{P,T}/RT$ versus C/C^* shows a broad range of cross-over concentrations signifying the relative inaccessibility of the asymptotic behavior for the scaling law exponents even with polymer molecular weights exceeding 10^6 g/mole. As the cooperative diffusion coefficient is also independent of polymer molecular weight, the slow characteristic time (D_s) becomes the only accessible parameter capable of revealing information on polymer molecular weight (or molecular clustering) in semidilute solutions. However, we should note that $\bar{D}_s$ $(\sim(M_n M_w)^{-1})$ differs from $\bar{D}_T$ $(\sim M_w^{-\alpha_D})$ in its averaging process even if eq. (9) is valid. Therefore, $\bar{D}_s$ and $\bar{D}_T$ behave differently in a polydisperse system. Similarly, the variance of $\bar{D}_s$, $\mu_2/\bar{\Gamma}_s^2$, provides a curious relationship to the molecular weight averages. In any case, analysis of D_s in a polydisperse system involves the use of cumulants method or multiexponential singular value decomposition technique in order to account for the non-single exponential behavior of $|g^{(1)}(\tau)|$.

In our analysis, we have noted that we can monitor the evolution of polymer formation, and in dilute solutions, measure many important molecular parameters of the polymer product, such as the weight-average molecular weight M_w, the z-average radius of gyration $\langle R_g^2\rangle_z^{1/2}$, second virial coefficients A_2 and k_d, the characteristic times associated with translation and its corresponding equivalent hydrodynamic radius R_h as well as estimates of the size (or molecular weight) distribution. In semidilute solutions, the accessible quantities, such as the osmotic compressibility $(\partial\pi/\partial C)_{P,T}$ and the cooperative diffusion coefficient D_c become independent of molecular weight. However, these quantities, while no longer properties of polymer molecular weight, can be used to compute polymer concentration if a correspondence relationship is known.

Assignment of very slow characteristic times as observed by QLS to self-

diffusive motions is open for discussion even though eq. (9) with appropriate variations in the concentration exponent, as shown in Table 3 for PMMA in MMA, is almost certainly applicable as an empirical equation which permits us to estimate some molecular properties of the polymer in semidilute solutions. It should be noted that in the present context we are mainly interesed in using exisiting known scattering techniques to monitor polymerization processes. Therefore, the interesting question on the exact nature of the slow mode in semidilute solutions can be settled as a separate issue. Nevertheless, we can point to the suggestion that from measurements of the concentration and molecular weight dependence of the slow mode we have a possibility to obtain additional information on the polymer product.

The interpretation and measurements on the cooperative diffusion coefficient may be more complex[25] because of the transient network lifetime.

There are two distinct elastic moduli in polymer solutions at semidilute concentrations:

$$D_c = [K_{os} + (4/3)G]/f \qquad (27)$$

where K_{os}, G, and f are, respectively, the osmotic modulus, the shear modulus and the frictional coefficient with concentration dependences of $K_{os} \sim C^3$, $G \sim C^2$ and $f \sim C^2$ in the theta region. This represents the second aspect of our studies, i.e., to use the polymerization data to investigate some aspects of the scaling theory.

Acknowledgements

BC wishes to thank Dr. G. Hagnauer of AMMRC, Watertown, Mass. for his encouragement and gratefully acknowledges the U.S. Army Research Office for support of this research project.

References

1. Chu, B. "Laser Light Scattering", Academic Press, N.Y. (1974); Berne, B. J. and Pecora, R., "Dynamic Light Scattering", Wiley, N.Y. (1976).

2. Chu, B., Fytas, G. and Zalczer, G., Macromolecules, 14, 395 (1981).

3. Chu, B. and Fytas, G., Macromolecules, 15, 561 (1982).

4. Chu, B. and Lee, D.-C., Macromolecules, 17, 926 (1984).

5. Chu, B. in "Scattering Techniques Applied to Supramolecular and Nonequilibrium Systems," ed. Sow-hsin Chen, Benjamin Chu, and Ralph Nossal (Plenum, New York, 1981), p. 231.

6. Chu, B., "Light Scattering Studies of Polymer Solution Dynamics," J. Polymer Sci., to be published.

7. Amis, E. J. and Han, C. C., Polymer, 23, 1403 (1983).

8. Amis, E. J., Janmey, P. A., Ferry, J. D. and Yu, H. Polym. Bull. 6, 13 (1991).

9. Amis, E. J., Janmey, P. A., Ferry, J. D. and Yu, H. Macromolecules, 16, 441 (1983).

10. Chu, B. in "Correlation Function Profile Analysis in Laser Light Scattering. I. General Review on Method of Data Analysis," *Proceedings of the NATO ASI on the Application of Laser Light Scattering to the Study of Biological Motions*, ed. J. C. Earnshaw and M. W. Steer, Plenum Press, 1983.

11. Ford, J. R. and Chu, B. "Correlation Function Profile Analysis in Laser Light Scattering. III. An Iterative Procedure," in Proceedings of the 5th International Conference on Photon Correlation Techniques in Fluid Mehanics, ed. E. O. Schulz-DuBois, Springer-Verlag, 1983. pp. 303-314.

12. Chu, B., Ford, J. R., and Pope J. "Light Scattering Characterization of Molecular Weight Distribution," Society of Plastic Engineers, ANTEC 83, 26, 547 (1983).

13. de Gennes, P. G., "Scaling Concepts in Polymer Physics," Cornell University Press, Ithaca, New York (1979).

14. Huglin, M. B. (ed.) "Light Scattering from Polymer Solutions," Academic Press, New York (1972).

15. O'Driscoll, K. F., Pure & Appl. Chem. 53, 617 (1981).

16. Balke, S. T. and Hamielec, A. E., J. Appl. Polym. Sci. 17, 905 (1973).

17. Tulig, T. J. and Tirrell, M., Macromolecules, 14, 1501 (1981).

18. Tulig, T. J. and Tirrell, M., Macromolecules, 15, 459 (1982).

19. Sawads, H., J. Polymer Science, B1, 305 (1963).

20. Oono, Y., Ohta, T. and Freed, K. F., J. Chem. Phys. 74, 6488 (1981).

21. Chu, B. and Nose, T., Macromolecules, 13, 122 (1980).

22. Koppel, D. E., J. Chem. Phys., 57, 4814 (1972).

23. Stockmayer, W. H., Schmidt, M., Pure & Appl. Chem. 54, 407 (1982).

24. DiNapoli, A., Chu, B. and Cha, C., Macromolecules, 15, 1174 (1982).

25. Brochard, F., J. Phys. (Paris), 44, 39 (1983).

END

FILMED

6-85

DTIC